Correlation Methods for the Centering, Rotation, and Alignment of Functional Brain Images

Larry Junck, John G. Moen, Gary D. Hutchins, Morton B. Brown, and David E. Kuhl

Department of Neurology, Division of Nuclear Medicine (Department of Internal Medicine), and Department of Biostatistics, University of Michigan, Ann Arbor, Michigan

Simple methods are described using correlation analysis to rotate functional brain images to a standard vertical orientation, identify the antero-posterior centerline, and align multiple images from the same brain level. Image rotation and centering are performed by determining the angle of rotation and centerline coordinate that result in maximal left-right correlation. Testing of this method on sets of multiple images acquired simultaneously through different brain levels suggests that the optimal rotation can be determined within 1° and the centerline within 0.3 mm. Spatial alignment of two or more images from the same brain level of a single subject is accomplished by finding the translation and rotation that yield the highest correlation between the images. Testing of the alignment method on sets of simultaneously acquired images at multiple brain levels suggests that the optimal translation can be determined within 0.45–0.69 mm and the optimal rotation within 0.8°. These methods are completely objective and can easily be automated.

J Nucl Med 1990; 31:1220–1276

Many different strategies are used for quantitative analysis of functional brain images such as those obtained with positron emission tomography (PET) and single-photon emission computed tomography (SPECT). We describe two methods using correlation analysis that serve as tools for the centering, rotation, and alignment of functional brain images prior to region of interest analysis.

Image Rotation and Centering

Rotation of images to a standard vertical orientation is useful for visual inspection and presentation of images, and it facilitates region of interest (ROI) analysis. In addition, many approaches to ROI analysis require either explicit or implicit identification of an antero-posterior centerline. Approaches used to determine cerebral cortex values from the two sides of the brain have included fitting a series of adjoining rectangles to the cortical rim (*1,2*), fitting a template containing predetermined ROIs to the brain (*3*), placing regions derived from an atlas of anatomical sections or magnetic resonance images (MRI) (*4,5,6*), and our own approach using an automated algorithm that locates the cortical rim and divides it into sectors (*7*). With any of these approaches, small degrees of image rotation result in inaccurate region placement, especially at the frontal and occipital poles. In addition, small shifts of the ROIs to the left or the right may result in substantial changes in left-right differences or asymmetry values.

We describe an objective approach for choosing an optimal angle of rotation to establish a standard vertical orientation and for identifying the anteroposterior centerline (axis of left-right symmetry, Fig. 1). This method relies on maximizing the correlation between values from the left and right sides of an image. This approach should improve the accuracy of analysis of data from the cerebral hemispheres, especially when comparison of values from left and right cerebral regions is required. We have previously described an application of image centering using this approach for analysis of images from normal subjects (*7*).

Alignment of Multiple Images

Some investigations require comparison of two or more image sets acquired at different times from the same level on a single subject. In some cases, the image sets may represent different physiologic variables (e.g., cerebral glucose metabolism, cerebral oxygen metabolism, and cerebral blood flow). In other cases, the image sets may represent the same variable obtained during different states of sensory, motor, or cognitive activation or at different stages of a disease. For comparison of values from these images, it is important that the brain be in nearly identical positions in the images. One approach to ensuring identical positioning is the use of a head holder with a tight-fitting face mask, but this approach is not available at all centers and may not be

Received Dec. 27, 1988; revision accepted Feb. 5, 1990.
For reprints contact: Larry Junck, MD, University of Michigan Hospitals, 1914/0316 Taubman Center, Ann Arbor, MI 48109.

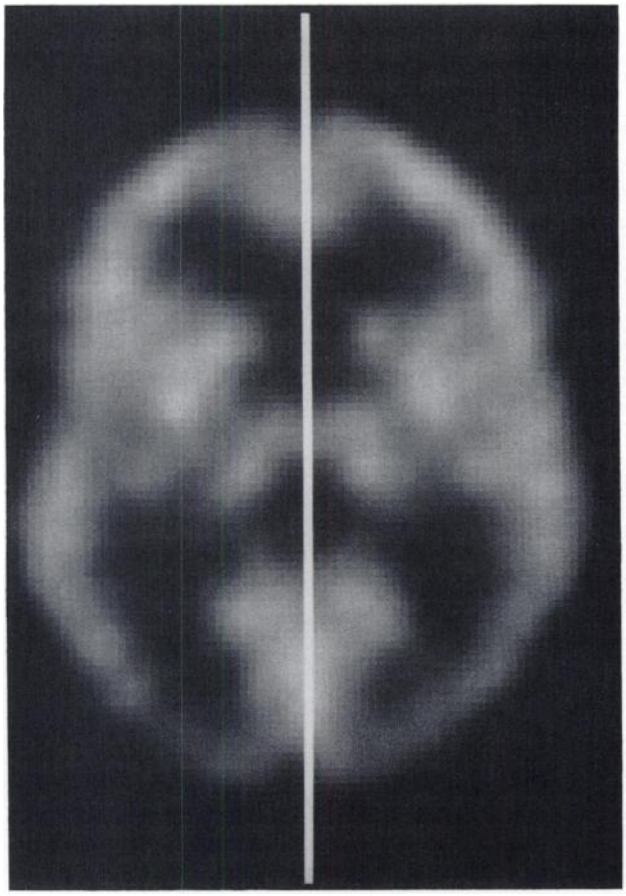

FIGURE 1
PET image of LCMRG with anteroposterior centerline (axis of left-right symmetry).

tolerated by some patients. In some situations, such as investigations performed during anesthesia (*8,9*), the use of a face mask may be difficult or medically contraindicated.

We describe an objective approach for alignment of two or more brain images along the left-right and anteroposterior axes as well as to the same angle of rotation about the rostro-caudal axis. This is performed by determining the translation and rotation of one image that maximizes the correlation between the pixel values in the two images.

MATERIALS AND METHODS

General Approach

The spatial coordinate X is defined as the left-right axis of the head, Y as the anteroposterior axis, and Z as the rostro-caudal axis. The angle of rotation about the Z axis is called θ.

The correlation r between two functional images W and V is calculated as:

$$r = \frac{\sum_i (W_i - \bar{W})(V_i - \bar{V})}{\sqrt{\sum_i (W_i - \bar{W})^2 \sum_i (V_i - \bar{V})^2}},$$

where W_i and V_i are the values in the ith pixel and $\bar{W}$ and $\bar{V}$ are the respective means over the entire images. However, when r is calculated over the entire image, the value of r will be strongly influenced by the amount of "empty space" included around the brain in the images, and thus the actual value of r is of little interest. The numerator of the above expression equals $\Sigma_i W_i V_i - n\bar{W}\bar{V}$ and is maximal whenever the cross product $\Sigma_i W_i V_i$ is maximal. The denominator of the above expression is the product of the standard deviations (s.d.s) of W_i and V_i, which are fixed over a given sample. Thus, r is maximal whenever the cross product is maximal. However, the cross product has the advantage of being insensitive to the amount of empty space included in the analysis. It is desirable to include pixels beyond the anatomical limits of the brain to increase the slope of the correlation function and improve the accuracy of detection of the peak value.

The approach we have taken is to calculate the cross product over the entire 24-cm image matrix. The cross product is calculated for a range of translations and rotations of one of the images. If the peak in the cross product is not included within the range selected, then the range is extended until the peak is identified. The optimal translation and rotation are those that yield the highest cross product.

Image Centering and Rotation

To determine the anteroposterior centerline of an image, six or seven copies of the image are rotated through various angles $\Delta\theta$ at 1-degree increments. A copy of each of these images is then flipped about the anteroposterior (Y) axis, translated in the X direction, and multiplied pixel-by-pixel by the unflipped copy to yield a product image. Summation of each product image over a large ROI encompassing the entire image defines the cross product. Calculation of the cross product over a range of translations ΔX and rotations $\Delta\theta$ yields the cross product surface, a function of ΔX and $\Delta\theta$. The peak of the cross-product surface determines the optimal rotation and centerline. Because translations of one pixel correspond to centerlines spaced at one-half pixel increments, the potential centerlines are spaced at one-half pixel increments. Because our system rotates images only at multiples of 1°, the optimal rotation can be determined to the nearest degree. For the purposes of this study, the optimal centerline and rotation were determined to greater accuracy by fitting a quadratic function (response surface) in ΔX and $\Delta\theta$ to the cross product surface and finding its peak. In our imaging system, image rotation involves interpolation, and cross products calculated from unrotated images tend to be slightly larger than cross products from rotated images. For this reason, the cross products at 0° rotation were eliminated from the fit.

Alignment of Multiple Images

To determine the optimal translation in the X and Y directions as well as the optimal rotation to align two images, ranges of potential translations and rotations are identified. One of the images is rotated, translated, and multiplied by the other image to yield a product image. Summation over the product image defines the cross product. Calculation of the cross product over a range of translations ΔX and ΔY and rotations $\Delta\theta$ gives the cross product surface, a function of ΔX, ΔY, and $\Delta\theta$. The peak of the cross-product surface defines the optimal translation to the nearest pixel and the optimal rotation to the nearest 1°. For the purposes of this study, the optimal centerline and rotation were determined to greater

accuracy by fitting a quadratic function (response surface) in ΔX, ΔY, and $\Delta\theta$ to the cross product surface and finding its peak. Cross products from unrotated images tended to be slightly larger than cross products from rotated images, and the cross products from unrotated images were therefore eliminated from the fit.

Testing the Methods

The above methods were tested on images of local cerebral metabolic rate for glucose (LCMRG) calculated from [^{18}F] fluorodeoxyglucose scans by the method of Phelps et al. (*10*) and images of local cerebral blood flow (LCBF) calculated from dynamic [^{15}O]H_2O scans using a modification of the weighted integral lookup table approach of Alpert et al. (*11*). The scans were performed using a PCT 4600A tomograph, which has an intrinsic resolution of ~1.1×1.1×0.95 cm. This tomograph simultaneously images five planes with center-to-center spacing of 1.15 cm. Patients were carefully aligned in the tomograph using laser beams in the planes of the cantho-meatal line and the cranial midline, but position along the anteroposterior axis was not rigorously controlled. LCMRG was measured in cerebral cortical regions using an automated algorithm that defines symmetrical ROIs in a 1.5 cm thick cortical ribbon (*7*). Left-right asymmetry was calculated as 100% (R − L)/[0.5 (R + L)].

To test the centering and rotation method, we identified LCMRG studies in which four planes through the cerebral hemispheres were imaged simultaneously. The optimal centerline and rotation were determined by curve fitting as described above, and values from the four planes were compared. To adjust for possible tilt in the images, a straight line was fitted by least squares to the centerlines of the four planes, and the deviation of the centers from the straight line was summarized by the root mean square (RMS) residual. The values were also compared with results of centering and rotation by eye. To identify the optimal centerline and rotation by eye, each image was separated from other images in the same set and intermixed with images from other subjects. A circumferential ellipse and anteroposterior centerline were overlain on the image as visual guides to centering and rotation.

On a larger number of LCMRG studies, the centering method was compared with two alternative methods, the center-of-gravity method and centering "by eye." The center-of-gravity method is largely objective, i.e., it requires only a minimum of judgment. An ellipse was fitted visually to each brain image, and a threshold was established at 33% of the mean value within the ellipse. All pixels above the threshold were assigned a constant arbitrary value, and all pixels below the threshold were set to zero. Occasionally the threshold was set at a value <33% to prevent values in or near the lateral ventricles from falling below the threshold, and occasionally it was set higher than 33% to prevent noise extending outside the brain contour from meeting the threshold. Centering by eye, a highly subjective approach, is described above.

We also tested the centering method using simulated PET scans derived from an MRI image at the level of the basal ganglia. Gray matter structures were set to a value four times that of white matter. Projections through the image were simulated for three detector geometries producing images with resolutions of 5, 10, and 15 mm (*12*). Gaussian noise appropriate to total image acquisitions of 0.5 to 4 million counts was added to the sinograms. At each rotation and count density, 500 reconstructed images were analyzed. On each image, the cross product was calculated as a function of ΔX, and a Gaussian function was fitted to the cross product curve to determine the centerline.

To test the alignment method, we analyzed LCBF studies in which five planes through the brain were scanned multiple times. The optimal translations ΔX and ΔY and the optimal rotation $\Delta\theta$ were determined in each plane by curve fitting. To adjust for a possible difference in tilt between the two image sets, straight lines were fitted by least squares to the translations ΔX and ΔY of the five planes, and the deviation of these values from the fitted lines were summarized by the RMS residuals.

RESULTS

Image Centering and Rotation

In 22 normal volunteers, the correlation method was applied to 37 sets of four adjacent planes through the cerebral hemispheres imaged simultaneously, formatted in a 128×128 matrix with 1.88 mm pixel dimensions. The centerline coordinate and optimal rotation were calculated by curve fitting. The results are presented in Table 1. Linear regressions among the centerlines of images within a set yielded slopes significantly different from zero ($p < 0.05$) in only 6 of 37 image sets, suggesting that the subjects usually had their heads positioned without significant tilt. The RMS residuals suggest that centering by correlation is significantly more accurate than centering by eye ($p < 0.001$) and has a potential accuracy of 0.3 mm or better. The results of centering by correlation agree well with those of centering by eye. The small but significant mean difference between the centers by correlation and those determined by eye, −0.56 mm, probably reflects an offset in our imaging system between the image plane and the overlay plane, and it highlights one of the problems that can occur with imaging by eye. The s.d. of rotations among four images in the same set suggests that the optimal rotation can be determined to an accuracy of ~1° by correlation and that the accuracy of rotation by correlation is approximately equal that of rotation by eye. The rotation by correlation agrees well with that chosen by eye.

The correlation method for centering was compared with the center of gravity method and the "eye" method on 410 planes of LCMRG scans from 41 normal subjects formatted in a 64×64 matrix with 3.75 mm pixel dimensions. No two methods ever disagreed by more than 0.5 pixels. The correlation method produced the same centerline as at least one of the other two methods in 96% of planes, while the center-of-gravity and eye methods produced the same centerline as at least one other method in 89% and 78%, respectively.

The centering method was applied to 1,135 planes of LCMRG scans from 143 patients and normal subjects.

TABLE 1
Tests of Correlation Analysis for Centering and Rotation of Normal PET Images*

	Centering ΔX	Rotation $\Delta\theta$
Standard deviations (s.d.) among sets of four images†		
s.d. of values by correlation	0.40 mm	0.98°
s.d. of values by correlation, rounded	0.44 mm‡	1.13°
s.d. of values obtained by eye	0.57 mm‡	0.92°
Root mean square (RMS) residuals among sets of four images§		
RMS residual by correlation	0.27 mm	—
RMS residual by correlation, rounded	0.31 mm¶	—
RMS residual of values obtained "by eye"	0.52 mm¶	—
Comparison of values by correlation with values by eye		
Mean difference, correlation - eye	−0.56 mm**	0.54°
s.d. of difference	0.55 mm	1.16°
Comparison of two interleaved sets of planes acquired sequentially††		
RMS difference between s.d.s by correlation	0.06 mm	0.50°
RMS difference between s.d.s by eye	0.27 mm	0.44°

* All analyses performed on 37 sets of LCMRG scans on 22 normal subjects.
† s.d. among centers or rotations of four planes imaged simultaneously.
‡ s.d. of centers by correlation (rounded to 0.5 pixel) is significantly smaller than s.d. of centers by eye by Wilcoxon signed rank test, $p < 0.01$.
§ Root mean square residual after linear regression (to correct for head tilt) among centers of four planes imaged simultaneously.
¶ RMS residual by correlation (rounded to 0.5 pixel) is significantly smaller than RMS residual by eye by Wilcoxon signed rank test, $p < 0.001$.
** Mean difference is significantly different from zero by t-test, $p < 0.001$.
†† Root mean square difference between s.d.s of interleaved sets, a measure of precision of the method, among 12 subjects.

The patients included those with olivopontocerebellar atrophy, Alzheimer's disease, progressive supranuclear palsy, and brain tumors. In every plane, the cross product curve had a single peak that defined a unique image centerline. The centerlines defined by the correlation method were acceptable to the eye in all patients including those with large brain tumors with a single exception. In that patient who had a brain tumor, superimposition of a hypermetabolic craniotomy flap with contralateral cerebral cortex led to an unacceptable centerline. The rotation method was also tried on scans from patients with markedly asymmetrical scans due to brain tumors, but in a few instances its results disagreed by as much as several degrees from the rotation chosen by eye.

With the simulated PET scans, the centerline X coordinate at various count densities ranged from 0.077 to 0.083 mm at 5 mm resolution, −0.074 to −0.070 mm at 10 mm resolution, and −0.026 to −0.015 mm at 15 mm resolution. Thus, resolution appeared to have a small influence on the center coordinate that was independent of count density. The s.d.s of the centerline coordinate are portrayed in Figure 2. The s.d. was virtually independent of image resolution but decreased with increasing numbers of counts in the images. With 3 million counts and 10 mm resolution, variables similar to those of the LCMRG scans analyzed in this study, the s.d. of the centerline coordinate was 0.045 mm, only slightly smaller than the precision estimated from comparison of interleaved sets of scans (Table 1).

To determine the impact of choice of centerline on the calculated asymmetry between left and right cortical regions, we analyzed 30 planes from LCMRG scans on 10 normals. Each plane was analyzed at the optimal rotation but with four different centerlines, separated by one-half pixel (0.94 mm). These four centerlines included the two best centerlines by correlation analysis and one additional centerline to the left and right of these two centerlines. The average change in asymmetry for the cerebral cortex from the entire hemisphere analyzed from one plane was 1.6% between the two best centerlines, 2.2% between the leftmost centerlines, and

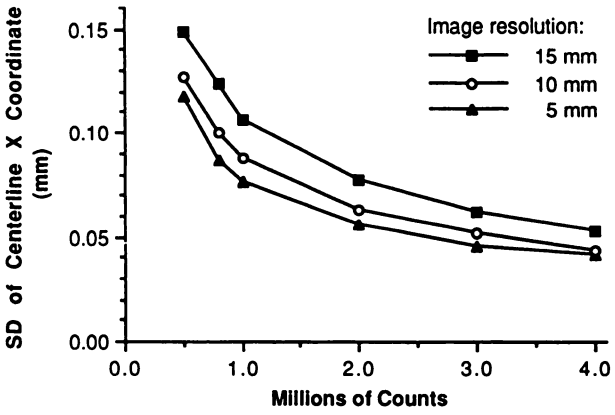

FIGURE 2
Standard deviation of centerline X coordinate as a function of image resolution and number of counts in image. Data are from simulations using an image derived from an MRI scan.

2.4% between the two rightmost centerlines. The average change in asymmetry for individual sectors of cerebral cortex (eight sectors per hemisphere) was 2.4% between the two best centerlines and 3.0% between either the two leftmost centerlines or the two rightmost centerlines. With each pair of centerlines, the centerline further to the left led to greater right-greater-than-left asymmetry than the centerline further to the right. From these values, it can be estimated that a 1-mm error in centerline coordinate results in ~ a 1.7%–2.5% error for whole hemisphere values and a 2.5%–3.2% error for sectors of cerebral cortex.

Alignment of Multiple Images

The correlation method was used to compare repeated LCBF scans on 28 patients. Among 8 normal elderly subjects, 9 patients with Parkinson's disease, and 6 with Alzheimer's disease, a set of scans performed during maximal auditory and visual stimulation was aligned with a set performed in the awake resting state. Among 5 patients with brain tumors, a scan performed during barbiturate anesthesia with hypocapnia was aligned with a scan in the awake resting state. The standard deviations of ΔX, ΔY and $\Delta\theta$ among the five planes in each image set are shown in Table 2, as are the RMS residuals for ΔX and ΔY after fitting the values from five planes to a straight line. The RMS residuals are measures of the variability of ΔX and ΔY that cannot be accounted for by a difference in head tilt between the two sets. The slope of ΔX as a function of Z was significantly different from zero ($p < 0.05$) in only 1 of 28 patients, and the slope of ΔY as a function of Z was significant in 6 cases. These findings suggest that differences between the two image sets in head tilt to one side or in the angle of the scan with respect to the canthomeatal line were infrequent.

DISCUSSION

Centering, rotation, and alignment by correlation analysis offer the advantage of complete objectivity, and these methods can readily be automated. In addition, centering by correlation appears to be significantly more accurate than centering by eye, as indicated by the fit of the centerlines from simultaneously acquired images to a straight line. Rotation by correlation, in contrast, appears equal in accuracy to rotation by eye, and thus one logical approach to image analysis would utilize rotation by eye, followed by centering by correlation. Centering and rotation by correlation work best on relatively symmetrical images including those from normal subjects and patients with degenerative neurological diseases, and caution must be used in applying these methods to images showing marked asymmetries due to focal brain disorders. In contrast, alignment of multiple images by correlation works well even on asymmetrical images, as exemplified by the images from brain tumor patients analyzed in this study.

The use of correlation analysis does not eliminate the need for careful positioning of the head or a reliable headholding system. Image centering by correlation analysis may identify small degrees of head tilt in the X direction as described in Results, but it does not provide a method for correcting the effects of tilt on the images. Centering and rotation by correlation analysis is undoubtedly less accurate when the brain is grossly tilted, and left-right comparisons of lateral structures including cerebral cortex are of less value with all but the smallest degrees of tilt. Similarly, the alignment method may identify differences between image sets in tilt in the X and Y directions, but it does not provide a means for correcting the effects of tilt on the images themselves. A headholder has the additional advantage of minimizing head movement during acquisition of individual images, a problem that correlation analysis cannot address. Even when a headholder is used, however, correlation analysis may be useful to define the optimal rotation and centerline and, unless the headholder restricts head movement to fractions of 1 mm, to align sequential images.

Correlation analysis appears to complement rather than compete with most other methods for image orientation and alignment. The method described by Levin, Pelizzari, and colleagues (*14,15*) for image alignment based on surface contours is capable of matching PET images with x-ray computed tomography (CT)

Tests of Correlation Analysis for Alignment of Multiple Images*

	ΔX	ΔY	$\Delta\sigma$
Standard deviations among sets of five images†			
s.d. of values by correlation	0.45 mm	0.69 mm	0.80°
RMS residuals among sets of five images‡			
RMS residual by correlation	0.38 mm	0.54 mm	—

* All analyses performed aligning two sets of LCBF images through the same levels of the brain on 28 patients.

† Standard deviation of translations or rotations determined by correlation among five planes imaged simultaneously.

‡ Root mean square residual after linear regression (to correct for any difference in head tilt between the two image sets) among translations of five planes imaged simultaneously.

and MRI images, something that the present method cannot accomplish. However, it requires an attenuation image for use with PET, and it cannot correct for head movement between the attenuation image and functional images. Furthermore, their method cannot be used with SPECT. The accuracy of this method for alignment of PET images with each other has not been reported to our knowledge, but phantom studies suggest an accuracy of ~1.8 mm for alignment of PET with MRI or CT. Maguire et al. (*16*) described an approach for alignment of multiple PET images by correlating the location of 7 to 10 landmarks identified on each image. Our approach does not require identification of landmarks, a process which is necessarily subjective, time-consuming, and inaccurate on PET and SPECT brain images. The MRI atlas method of Evans (*6*) permits anatomic localization, which the present method cannot do, but it also relies on selection of landmarks for image alignment. The stereotactic method of Fox et al. (*5*) also permits anatomic localization, but it does not provide an approach for alignment of PET images, relying instead on the headholder to maintain the same head position.

The correlation method can be expected to work best on images such as LCMRG and LCBF scans which have a large dynamic range, i.e., areas of high and low radioactivity corresponding to various structures in the brain. Its accuracy for centering and rotation of other types of images will depend on the dynamic range of those images. Its accuracy for aligning one type of functional image with another will undoubtedly depend on the similarity of the patterns in the two types of images. Our studies using simulated PET images suggests that image noise is more important than image resolution as a determinant of the accuracy of the correlation methods. We have used the correlation approach only for analysis of two-dimensional planar images, but it should perform equally well or better on three-dimensional data sets.

Image Centering and Rotation

Ideally, it would be desirable to compare the accuracy of centering and rotation by correlation analysis with a gold standard method, but no such standard exists. The use of CT or MRI to locate midline anatomic landmarks such as the falx cerebri does not provide a satisfactory standard because the curvature of the falx may be as great as several millimeters. Furthermore, when anatomic asymmetries are present, an approach that utilizes only center landmarks such as the falx does not necessarily result in a centerline located midway between more lateral structures. The approach using correlation analysis utilizes *all* the information from a functional brain image, and it may be argued that this results in the best single choice of centerline for analysis of any portion of the image.

Estimates of the potential accuracy of this approach are the RMS residual (after correction for tilt) of 0.27 mm for centering and the s.d. among rotations of interleaved image sets of 0.98°. These figures may be overestimates because they do not account for any curvature in the center plane of the brain. An approach to estimation of the precision of these methods, the RMS difference between the s.d.s among the centers and rotations of interleaved images, suggests a precision as great as 0.06 mm for centering and 0.50° for rotation. In actual application of this method, the centerline coordinate will usually be determined to the nearest half-pixel, and the error introduced by rounding to the nearest half-pixel will range from zero to one-quarter pixel and will average one-eighth pixel. This error resulting from rounding will in most cases be greater than the error introduced by the correlation process. Using our imaging system with 64×64 matrix images, this corresponds to an average error in left-right asymmetry of cerebral cortex resulting from centerline coordinate roundoff of 0.8%–1.2% for the entire hemisphere and 1.2%–1.5% for cortical subregions. These figures may differ with other approaches to image analysis. Nonetheless, it is clear that accurate centering is required to assess small degrees of asymmetry.

Alignment of Multiple Images

The use of correlation analysis for alignment of multiple images was described by Hibbard et al. (*13*), who used it to align sequential sections from autoradiographic rodent brain images. Anatomic differences between brain levels and anatomic distortions occurring during brain sectioning confound this application of correlation analysis. Application to PET images is free of these sources of error and represents a more ideal use of correlation analysis.

The gold standard for alignment of multiple PET images by correlation analysis would be a headholding method that permits no movement in X or Y and no rotation. However, the best available headholding methods probably permit 1 mm or more movement. Our estimates of the best possible accuracy of correlation analysis for alignment of multiple images come from sets of simultaneously acquired LCBF images, where we found the RMS residual for translation (after correction for head tilt) to be 0.38 mm for X and 0.54 mm for Y, and the s.d. for rotation was 0.80°. In actual application of this method, the translation in each direction will usually be determined to the nearest pixel, and the average error introduced by rounding to the nearest pixel is one quarter of the pixel dimension. The average error introduced by rounding to the nearest 1° will be 0.25°.

ACKNOWLEDGMENTS

The authors thank Dr. Robert A. Koeppe for advice and criticism, Drs. Sid Gilman and Normal L. Foster for permis-

sion to test these methods on images from their patients, and Ms. Virginia Rogers for implementing these methods on our image analysis system. We also thank the staff of the Division of Nuclear Medicine for their assistance with the PET investigations.

This work was supported by NIH grant no. NS 15655. Dr. Junck is the recipient of Teacher-Investigator Development Award no. 5 K07 NS00908 from NIH. A portion of Mr. Moen's work was supported by the Kughn Clinical Research Center at the University of Michigan through the Medical Student Research Program. Dr. Brown's effort was also partially supported by the Kughn Clinical Research Center through NIH grant no. MOI RR00042.

REFERENCES

1. Mazziotta JC, Phelps ME, Carson RE, Kuhl DE. Tomographic mapping of human cerebral metabolism: Sensory deprivation. *Ann Neurol* 1982; 12:435–444.
2. Duara R, Margolin RA, Robertson-Tchabo EA, et al. Cerebral glucose utilization, as measured with positron emission tomography in 21 resting healthy men between the ages of 21 and 83 years. *Brain* 1983; 106:761–775.
3. Dann R, Muehllehner G, Rosenquist A. Computer-aided data analysis of ECT data. *J Nucl Med* 1983; 24:82.
4. Horwitz B, Duara R, Rapoport SI. Age differences in correlations between regional cerebral metabolic rates for glucose. *Ann Neurol* 1986; 19:60–67.
5. Fox PT, Perlmutter JS, Raichle ME. A stereotactic method of anatomical localization for positron emission tomography. *J Comput Assist Tomogr* 1985; 9:141–153.
6. Evans AC, Beil C, Marrett S, Thompson CJ, Hakim A. Anatomical-functional correlation using an adjustable MRI-based region of interest atlas with positron emission tomography. *J Cereb Blood Flow Metab* 1988; 8:513–530.
7. Junck L, Gilman S, Rothley JR, Betley A, Koeppe RA, Hichwa RD. A relationship between metabolism in frontal lobes and cerebellum in normal subjects studied with PET. *J Cereb Blood Flow Metab* 1988; 8:774–782.
8. Blacklock JB, Oldfield EH, Di Chiro G, Tran D, Theodore W, Wright DC, Larson SM. Effect of barbiturate coma on glucose utilization in normal brain versus gliomas: Positron emission tomography studies. *J Neurosurg* 1987; 67:71–75.
9. Junck L, Van Der Spek ASL, Aldrich MS, Gebarski SS, Greenberg HS. Effects of barbiturate anesthesia and hyperventilation on CBF in patients with brain tumors. In: JT Hoff, Betz AL, eds. *Intracranial pressure VII: proceedings of the seventh international symposium on intracranial pressure.* Berlin: Springer Verlag; 1989: 891–893.
10. Phelps ME, Huang SC, Hoffman EJ, Selin C, Sokoloff L, Kuhl D. Tomographic measurement of local cerebral glucose metabolic rate in humans with (F-18)2-fluoro-2-deoxy-D-glucose: validation of method. *Ann Neurol* 1979; 6:371–388.
11. Alpert NM, Eriksson L, Chang JY, et al. Strategy for the measurement of regional cerebral blood flow using short-lived tracers and emission tomography. *J Cereb Blood Flow Metab* 1984; 4:28–34.
12. Hutchins GD, Penney JB, Young AB, Morten B, Koeppe RA. Evaluation of PET feasibility studies employing autoradiography, MRI, and computer simulated positron emission tomography. *J Nucl Med* 1988; 29:774.
13. Hibbard LS, McGlone JS, Davis DW, Hawkins RA. Three-dimensional representation and analysis of brain energy metabolism. *Science* 1987; 236:1641–1646.
14. Levin DN, Pelizzari CA, Chen GTY, Chen C-T, Cooper MD. Retrospective geometric correlation of MR, CT, and PET images. *Radiology* 1988; 169:817–823.
15. Pelizzari CA, Chen GTY, Spelbring DR, Weichselbaum RR, Chin C-T. Accurate three-dimensional registration of CT, PET, and/or MR images of the brain. *J Comp Assist Tomog* 1989; 13:20–26.
16. Maguire GQ, Noz ME, Lee EM, Schimpf JH. Correlation methods for tomographic images using two and three dimensional techniques. In: Bacharach SL, ed. *Information processing in medical imaging: proceedings of the ninth international conference on information processing in medical imaging.* Dordrecht: Martinus Nijhoff; 1989:266–278.